Coordination of Cu_B in Reduced and CO-Liganded States of Cytochrome bo_3 from *Escherichia coli*. Is Chloride Ion a Cofactor?†

Martina Ralle,‡ Marina L. Verkhovskaya,§ Joel E. Morgan,§ Michael I. Verkhovsky,§ Mårten Wikström,§ and Ninian J. Blackburn*,‡

Department of Biochemistry and Molecular Biology, Oregon Graduate Institute of Science and Technology, P.O. Box 91000, Portland, Oregon 97291, and Helsinki Bioenergetics Group, Institute of Biomedical Sciences, Department of Medical Chemistry and Biocentrum Helsinki, University of Helsinki, 00014 Helsinki, Finland

Received December 8, 1998; Revised Manuscript Received March 2, 1999

ABSTRACT: The ubiquinol oxidase cytochrome bo_3 from *Escherichia coli* is one of the respiratory heme−copper oxidases which catalyze the reduction of O_2 to water linked to translocation of protons across the bacterial or mitochondrial membrane. We have studied the structure of the Cu_B site in the binuclear heme−copper center of O_2 reduction by EXAFS spectroscopy in the fully reduced state of this enzyme, as well as in the reduced CO-liganded states where CO is bound either to the heme iron or to Cu_B. We find that, in the reduced enzyme, Cu_B is coordinated by one weakly bound and two strongly bound histidine imidazoles at Cu−N distances of 2.10 and 1.92 Å, respectively, and that an additional feature at 2.54 Å is due to a highly ordered water molecule that might be weakly associated with the copper. Unexpectedly, the binding of CO to heme iron is found to result in a major conformational change at Cu_B, which now binds only two equidistant histidine imidazoles at 1.95 Å and a chloride ion at 2.25 Å, with elimination of the water molecule and one of the histidines. Attempts to remove the chloride from the enzyme by extensive dialysis did not change this finding, nor did substitution of chloride with bromide. Photolysis of CO bound to the heme iron is known to cause the CO to bind to Cu_B in a very fast reaction and to remain bound to Cu_B at low temperatures. In this state, we indeed find the CO to be bound to Cu_B at a Cu−C distance of 1.85 Å, with chloride still bound at 2.25 Å and the two histidine imidazoles at a Cu−N distance of 2.01 Å. These results suggest that reduction of the binuclear site weakens the bond between Cu_B and one of its three histidine imidazole ligands, and that binding of CO to the reduced binuclear site causes a major structural change in Cu_B in which one histidine ligand is lost and replaced by a chloride ion. Whether chloride is a cofactor in this enzyme is discussed.

The structurally and functionally related heme−copper oxidases catalyze cell respiration in prokaryotes and in the mitochondria of eukaryotic cells, and conserve energy by linking this exergonic reaction to proton translocation across the respective membrane (*1*). The largest subunit in all these enzymes (subunit I) contains a heme iron−copper reaction site (the binuclear center), in which the reduction of oxygen to water takes place, and a low-spin heme which transfers electrons to this center. In the ubiquinol-oxidizing cytochrome bo_3 from *Escherichia coli*, the binuclear center contains heme O, while heme B (protoheme) is usually inserted in the low-spin heme site (*2*, *3*). The copper in the binuclear site is usually termed Cu_B.[1] The crystal structures of two members of the heme−copper oxidase superfamily have been elucidated at atomic resolution (*4*−*7*), and it appears likely that the structure of cytochrome bo_3 is very similar (*8*). A bimetallic mixed-valence Cu_A center in subunit II accepts electrons from cytochrome *c* and donates them further to the low-spin heme in the cytochrome *c* oxidases. In contrast, the ubiquinol oxidases lack the Cu_A center (*9*), and the low-spin heme receives electrons directly from ubiquinol. The presence of only one copper (Cu_B) in the quinol oxidases makes them better suited for copper XAS studies of the binuclear site.

The structure of the binuclear oxygen-reducing site is of obvious interest with respect to the mechanism of O_2 reduction to water. It was established by site-specific mutagenesis experiments (*10*) and confirmed by the X-ray work (cf. above) that the oxygen-binding heme is ligated proximally by a histidine residue from transmembrane helix X in subunit I. Likewise, mutagenesis experiments had predicted that Cu_B has one histidine ligand from helix VI and two from helix VII, as also confirmed by the X-ray structures. A combined copper EXAFS and ENDOR study

† This research was supported by Grant GM-54803 from the National Institutes of Health (to N.J.B.) and by grants from the Academy of Finland, the University of Helsinki, and the Sigrid Juselius Foundation (to M.W.).

* To whom correspondence should be addressed: Department of Biochemistry and Molecular Biology, Oregon Graduate Institute of Science and Technology, P.O. Box 91000, Portland, OR 97291-1000. Telephone: (503) 748-1384. Fax: (503) 748-1464. E-mail: ninian@bmb.ogi.edu.

‡ Oregon Graduate Institute of Science and Technology.

§ University of Helsinki.

[1] Abbreviations: Cu_B, copper of the binuclear oxygen-binding site; DW, Debye−Waller; EXAFS, extended X-ray absorption fine structure; Fe_{o3}, iron of the oxygen-binding heme in cytochrome bo_3; FT, Fourier transform; IR, infrared; XAS, X-ray absorption spectroscopy.

10.1021/bi982885l CCC: $18.00
Published on Web 05/11/1999

(*11*) of the quinol oxidase from *Bacillus subtilis* also showed three histidine ligands to Cu_B, but further indicated the presence of a fourth ligand with exchangeable proton(s), which was assigned as either water or OH^-. As judged from the ligand structure of the Cu_B site in the crystallographic models, this fourth oxygenous ligand would have to point obliquely toward the heme and could well be involved in the formation of an intermetal ligand bridge, which has long been postulated to explain the strong magnetic coupling between the two metals of the binuclear site (*12*). However, the heme Fe−Cu_B distances from the crystallographic data are too long to allow for this ligand alone to bridge the two metals, and the exact nature of the intermetal connectivity remains elusive.

Yoshikawa et al. (*13*) recently reported electron density between the heme iron and Cu_B in the oxidized cytochrome aa_3 from bovine heart mitochondria. They interpreted this density to be due to a bridging peroxide, but this is difficult to accept since several groups have reported that full reduction of the oxidized cytochrome *c* oxidase requires no more than four electrons (*14, 15*). Six electrons would be expected to be required to fully reduce the enzyme if peroxide were bound to the binuclear site. On the other hand, the electron density might also be consistent with an OH^- (or water) ligand of Cu_B (cf. above) and a water or another weak field ligand coordinated to the distal heme iron site. In such a case, an interaction between the iron-bound weak field ligand and the copper-bound OH^- (or water) would have to mediate the magnetic coupling.

Carbon monoxide has long been known to bind to the heme of the binuclear site in the reduced heme−copper oxidases. Photolysis of the reduced CO-bound enzyme at low temperatures results in dislocation of the iron-bound CO to Cu_B where it can be recognized by the specific C≡O stretch at ∼2065 cm^{-1} due to CO bound to copper (*16*). At room temperature, photodissociation of CO from heme iron and its subsequent binding at Cu_B is an extremely fast reaction, and then CO remains bound to Cu_B only for ∼1.5−2 μs (*17, 18*). After this, CO dissociates from the binuclear site and rebinds to heme iron via Cu_B at a much slower rate (*19*). More recently, Puustinen et al. (*20*) showed that the dislocation of CO from heme iron to Cu_B by photolysis at 80 K also results in perturbation of the conserved, protonated Glu-286 residue in cytochrome bo_3 of *E. coli*, which resides 11−12 Å from the binuclear center. This prompted us to explore the structure of the Cu_B site in the reduced and the reduced CO-treated enzyme by X-ray absorption spectroscopy. Meanwhile, Yoshikawa et al. (*13*) have reported the crystallographic structure of the reduced bovine enzyme in the presence and absence of CO. While they did not find any significant changes in the structure of Cu_B relative to the fully oxidized enzyme, we find a dramatic and somewhat unexpected change, especially upon addition of CO, which involves dissociation of one of the Cu_B histidine ligands and its replacement by chloride.

EXPERIMENTAL PROCEDURES

Sample Preparation and Analysis

Samples for EXAFS Spectroscopy. Enzyme samples were made anaerobic by repeated flushing with argon on a vacuum line (*21*). They were then reduced by addition of ascorbate (7 mM) and phenazine methosulfate (0.7 mM), followed by addition of glycerol to 21% (v/v). The bromide-containing sample that had been treated to remove loosely bound chloride (see below) included 28 mM NaBr. Samples were then transferred anaerobically to the EXAFS cells using gastight syringes from Hamilton (Reno, NV), and then removed from the anaerobic container and frozen promptly in liquid nitrogen. The three samples without bromide were all prepared together as a batch. After reduction and addition of glycerol, the enzyme for the reduced uncarbonylated EXAFS sample ("reduced") was removed and frozen. Carbon monoxide was then added to the remaining enzyme, and the remaining two samples were prepared, care being taken to keep one of them ("CO dark") in the dark. The other sample ("CO photolyzed") was placed in a liquid nitrogen-filled finger dewar and illuminated for several minutes using a slide projector. The bromide-containing sample was prepared separately.

Removal of Loosely Bound Cl^- and Determination of the Amount of Cl^- Remaining Strongly Bound to the Enzyme. One milliliter of enzyme solution (∼0.2−0.3 mM) was dialyzed against medium containing 0.4 M mannitol, 10 mM HEPES/KOH (pH 7.5), and 0.05% dodecyl maltoside in three steps: (i) 250 mL for 4 h, (ii) 250 mL for 4 h, and (iii) 500 mL overnight. After the overnight dialysis, the Cl^- concentration in the dialysis medium was <10 μM, but significantly higher (∼100 μM) within the dialysis bag, suggesting that the enzyme indeed binds chloride tightly. The amount of residual tightly bound Cl^- was determined as follows. Fifty microliters of oxidase solution (∼0.3 mM enzyme) from the EXAFS tube (after the EXAFS experiments) was treated with acid acetone (0.45 mL of acetone and 1.5 μL of 65% HNO_3) to extract the hemes. The protein was sedimented and the pellet discarded. The acetone/water mixture was evaporated from the supernatant in a vacuum concentrator. Water (0.2 mL) was added; the sample was shaken and centrifuged (12 000 rpm for 10 min in an Eppendorf centrifuge), and the heme pellet was discarded. The optical spectrum of the supernatant containing some remaining heme was taken as a baseline. The chloride assay kit (Spectroquant 14755) reagents were then added, and the spectrum was re-recorded. The chloride concentration was determined from the difference between these spectra.

X-ray Absorption (XAS) Data Collection and Analysis

XAS data were collected at the Stanford Synchrotron Radiation Laboratory (SSRL) on beam line 7.3, operating at 3.0 GeV with beam currents between 100 and 50 mA. A Si220 monochromator with 1.2 mm slits was used to provide monochromatic radiation in the 8.8−10 keV energy range. The monochromator was detuned 50% (at an energy of 9713 eV, corresponding to the end of the scan) to reject harmonics. The protein samples were measured as frozen glasses in 21% glycerol at 11−14 K in the fluorescence mode using a 13-element Ge detector. To avoid detector saturation, the count rate of each detector channel was kept below 100 kHz by adjusting the hutch entrance slits or by moving the detector in or out from the cryostat windows. Under these conditions, no dead time correction was necessary. The summed data for each detector were then inspected, and only those channels that gave high-quality backgrounds free from

glitches, drop outs, or scatter peaks were included in the final average.

Raw data were averaged, background-subtracted, and normalized to the smoothly varying background atomic absorption using the EXAFS data reduction package EXAFSPAK (*22*). Energy calibration was achieved by reference to the first inflection point of a copper foil (8980.3 eV) placed between the second and third ion chambers. In any series of scans, the measured energy of the first inflection of the copper foil spectrum varied by less than 1 eV. Averaged EXAFS data were referenced to the copper calibration of the first scan of a series, since the energy drift in any series of scans was too small to perturb the EXAFS oscillations. However, for edge studies, there was sufficient energy drift over the duration of the scans to lead to broadening of the edge features. To avoid this, measurements of Cu K-absorption edges were taken as a single scan for each sample in increments of 0.2 eV per point and with 2 s count rates per point in the energy range of 8960−9020 eV.

Two data sets were collected for each sample in April 1998 and July 1998. The samples measured in April 1998 were prepared without special precautions to remove adventitously bound chloride ion. The number of scans for each sample was as follows: 27 scans for fully reduced unliganded cytochrome bo_3, 19 scans for reduced bo_3 + CO in the dark, and 21 scans for reduced bo_3 + CO photolyzed. The samples measured in July 1998 were treated to minimize the Cl^- concentration as described above. The number of scans for each sample was as follows: 25 scans for fully reduced unliganded cytochrome bo_3, 29 scans for reduced bo_3 + CO in the dark, 28 scans for reduced bo_3 + CO photolyzed, and 30 scans for reduced bo_3 + CO + Br^- in the dark. Inspection of the data showed that no spectral changes occurred during data collection as the result of radiation damage or photoredox processes.

Data analysis was carried out with the least-squares curve-fitting program EXCURV98, which utilizes full curved-wave calculations as described by Gurman and co-workers (*23*−*26*). The application to metalloprotein systems, and particularly the treatment of imidazole rings from histidine residues and of linearly coordinated carbonyl groups by multiple-scattering analysis, has been described in detail in previous papers from this laboratory (*27*−*30*). The parameters refined in the fit were as follows: E_0, the photoelectron energy threshold; R_i, the distance from Cu to atom i; and $2\sigma_i^2$, the Debye−Waller (DW) term for atom i. The coordination numbers were also allowed to vary but, unless otherwise stated, were constrained to produce DW factors within reasonable limits (first shell, $0 < 2\sigma^2 < 0.01$; second shell, greater than or equal to the first shell). The goodness of fit was judged by reference to a goodness of fit parameter F, defined as

$$F^2 = \frac{1}{N}\sum_{i=1}^{n} k_6(\text{data}_i - \text{model}_i)^2$$

RESULTS

We have used X-ray absorption spectrosocopy to examine the structure of the Cu_B center of cytochrome bo_3 quinol oxidase in the fully reduced protein, as well as coordination changes at Cu_B which accompany binding of CO to the reduced enzyme and subsequent photolysis. This chemistry has been previously characterized as involving binding of CO to ferrous heme iron, followed by the photolytic dissociation of CO from the heme iron and rebinding at Cu_B as a Cu_B(I)−carbonyl with a ν(C≡O) of around 2065 cm^{-1} (see the introductory section). Our findings are unprecedented in that we report unambiguous evidence that a chloride ion is involved in the process and that it mediates histidine dissociation from the copper center as a central element of the reaction chemistry. Given the novelty of these data and the somewhat variable nature of cytochrome oxidase preparations, it was first important to test the reproducibility of the data using two independent sets of samples collected in two different beam time sessions at SSRL.

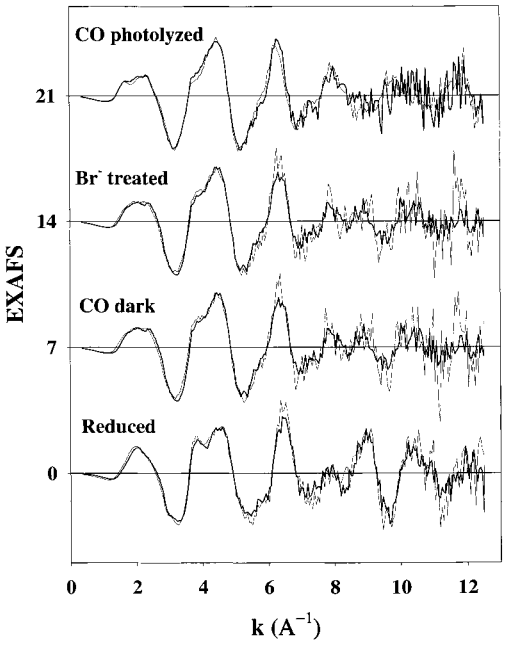

FIGURE 1: Reproducibility of background-subtracted EXAFS data. Pairs of spectra from bottom to top are as follows: untreated (thick line) vs low chloride (thin line) data for fully reduced bo_3, untreated (thick line) vs low chloride (thin line) data for dark-carbonylated bo_3, untreated (thick line) vs bromide-treated (thin line) data for dark-carbonylated bo_3, and untreated (thick line) vs low chloride (thin line) data for photolyzed bo_3.

In Figure 1, we compare the raw background-subtracted EXAFS data for the samples used in the study. The thick traces represent data collected in April 1998 from samples prepared with no precautions to exclude chloride; the thin traces represent data collected in July 1998 from samples which had been treated to remove excess (adventitious) chloride (termed low Cl). The pairs of spectra represent (from bottom to top): fully reduced cytochrome bo_3, normal Cl versus low Cl; reduced bo_3 + CO in the dark (CO on heme iron), normal Cl versus low Cl; reduced bo_3 + CO in the dark, normal Cl versus Br-treated data; and reduced bo_3 + CO after photolysis (CO on Cu_B), normal Cl versus low Cl. The reproducibility of the data is outstanding and in all cases exceeds the noise level. This provides confidence that all of the EXAFS and Fourier transform features (above the noise level) are real and structurally significant. Since the April data have a somewhat better signal-to-noise ratio, we have used these for further analysis.

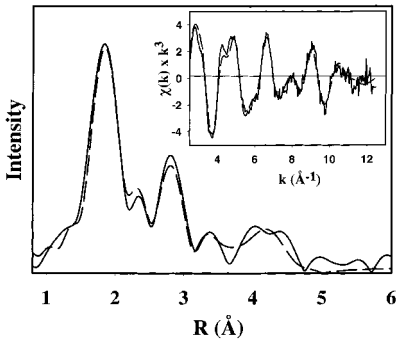

FIGURE 2: Experimental (solid lines) vs simulated (dashed lines) Fourier transform and EXAFS (inset) for fully reduced cytochrome bo_3 with multiple-scattering contributions from two equidistant histidines (parameters listed in Table 1).

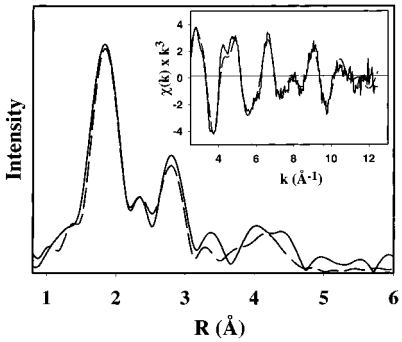

FIGURE 3: Experimental (solid lines) vs simulated (dashed lines) Fourier transform and EXAFS (inset) for fully reduced cytochrome bo_3 with multiple-scattering contributions from two equidistant histidines and a third more distant histidine with additional shells (parameters listed in Table 2).

Figure 2 shows experimental and simulated Fourier transform and EXAFS data (inset) for the fully reduced cytochrome bo_3. Reference to the published crystal structures of oxidized cytochrome aa_3 from bovine heart mitochondria (*6*, *7*, *13*) and from *Paracoccus denitrificans* (*4*, *5*) suggests that the Cu_B center should be coordinated to three histidine residues with no contributions from additional scatterers. The EXAFS spectral characteristics of Cu(II) and Cu(I) coordinated to three histidines have been well studied by XAS (*11*, *27*, *29*, *31*−*33*). Equidistant histidine ligation is expected to give rise to a simple spectrum, with an intense first shell peak (Cu−N_α, 1.90−2.0 Å phase-corrected) and two weaker peaks due to Cu−C_β (≈3.0 Å) and C_γ/N_γ (≈4.2 Å), respectively.

The data for the fully reduced cytochrome bo_3, although highly reproducible, are significantly more complex than expected for such a simple three-histidine-type spectrum. They exhibit a significant broadening of the first shell in the FT and a distinct, well-resolved peak at ∼2.5 Å (phase-corrected). All attempts to fit the data with a model involving two or three histidines at a single distance totally failed to reproduce either of these novel features. Thus, we examined alternatives in which the histidine shell was split with two shells of Cu−N(imid) distances contributing to the first peak in the FT.

First-shell Fourier-filtered data (not shown) were used to estimate the splitting of the first shell. Next, the single- and multiple-scattering contributions of the imidazole outer shells were included. To ensure accuracy, the outer shell distances and imidazole ring geometry were generated by molecular modeling using the builder module of INSIGHT 3.0 (Molecular Simulations Inc., San Diego, CA). A model of the copper center with a single coordinated imidazole was built first and the Cu−N first-shell bond length adjusted to be close to the EXAFS-derived bond length (as determined by first-shell analysis using Fourier-filtered data). This model was then converted into molecular coordinates and read into EXCURV98 to provide a single Cu−imidazole unit with the correct geometry. The coordination number of this unit was then set within the EXAFS program. Least-squares minimization was performed, varying only the Cu−N(imid) first-shell distance (R), its DW factor, and E_0, the photoelectron threshold energy. Finally, the C_β and C_γ/N_γ shells were allowed to minimize, but were constrained to remain within ∼0.1 Å of the initially chosen geometry. This latter process was found to be crucial in obtaining good fits to all of the data reported herein, and almost certainly reflects the real tendency of coordinated imidazole rings to distort from ideal geometries in response to tertiary structural constraints of the polypeptide fold. As expected, this analysis required the first shell to be split into two shells, two Cu−N(imid) at 1.92 Å and one Cu−N/O at 2.09 Å. Figure 2 shows the best fit ($F = 0.46$) that was obtained and includes outer shell single- and multiple-scattering contributions from two imidazoles at 1.92 Å (but excludes any multiple scattering arising from a 2.1 or 2.5 Å Cu−histidine bond). To fit the feature at ∼2.5 Å, it was absolutely necessary to include a shell of one Cu−O/N at 2.54 Å. In addition, two additional single-scattering shells of two carbon atoms each appeared to be present at 3.01 and 3.28 Å, respectively. The parameters used in this fit are listed in Table 1.

The structural identity of Cu_B in fully reduced cytochrome bo_3 thus depends on the interpretation of the 2.1 and 2.5 Å shells. It is reasonable to infer that one of these is derived from the third histidine ligand, while the other is most likely derived from a coordinated or highly ordered water molecule residing in the binuclear metal site pocket. The need to include additional low-Z (O, N, or C) shells at 3.01 and 3.28 Å suggests the presence of outer shell scattering from the third imidazole at a distance consistent with a Cu−N_α distance of 2.1 Å. As a test of this interpretation, the 2.1 Å scatterer was treated as a histidine ligand, and its single- and multiple-scattering contributions from all outer shell atoms of the imidazole ring were added to the fit. This produced the fit shown in Figure 3 with the parameters listed in Table 2. The fit is not as good as judged by an F value of 0.59, but is visually equivalent to the single-histidine fit. In particular, the additional shells of single-scattering C atoms are now partially accounted for by the two C_β atoms of the 2.10 Å Cu−N(his) imidazole ring at their appropriate distance of 3.10 Å. This fit still contains one additional C at ∼3 Å, not associated with histidine multiple scattering which we believe originates from the methylene C atom of the N_δ-coordinated H240 (bovine numbering). The rather strong scattering from this C could arise from the very rigid anchoring of the imidazole ring via the N_ϵ−Y244 cross-link (*13*). The two short (1.92 Å) histidine ligands have normal outer shell DW terms, but the long histidine has very weak outer shell scattering, suggesting multiple conformations or disorder.

It thus appears probable that fully reduced cytochrome bo_3 contains two strongly bound and one weakly bound imida-

Table 1: Parameters Used To Simulate the EXAFS and Fourier Transform of the Fully Reduced Cytochrome bo_3, Including Multiple Scattering from a Single Shell of Imidazole Scatterers[a]

first shell			outer shells			
shell (X)	R (Å)	$2\sigma^2$ (Å^2)	shell (Y)	R (Å)	∠Cu−X−Y (deg)	$2\sigma^2$ (Å^2)
			$F = 0.460$, $E_0 = -3.98$ eV			
2 N_α (imid)	1.92	0.0080	2 C_β (imid)	2.92	235	0.0100
			2 C_β (imid)	2.85	125	0.0100
			2 C_γ/N_γ (imid)	4.09	201	0.0165
			2 C_γ/N_γ (imid)	4.22	164	0.0165
1 N_α (imid)	2.09	0.0063	2 C	3.01		0.0080
1 O (solv)	2.54	0.0050	2 C	3.28		0.0200

[a] Estimated errors in distances are ±0.01 Å for the first shell and ±0.03 Å for outer shells. Estimated errors in coordination numbers are ±25%. Estimated errors in angles are ±5°. ∠Cu−X−Y represents the angle between the first-shell scatterer (X) and the outer shell scatterer (Y).

Table 2: Parameters Used To Simulate the EXAFS and Fourier Transform of the Fully Reduced Cytochrome bo_3 with Two Inequivalent Sets of Histidine Ligands[a]

first shell			outer shells			
shell (X)	R (Å)	$2\sigma^2$ (Å^2)	shell (Y)	R (Å)	∠Cu−X−Y (deg)	$2\sigma^2$ (Å^2)
			$F = 0.59$, $E_0 = -4.19$ eV			
2 N_α (imid)	1.92	0.0080	2 C_β (imid)	2.89	233	0.0095
			2 C_β (imid)	2.92	127	0.0095
			2 C_γ/N_γ (imid)	4.09	164	0.0200
			2 C_γ/N_γ (imid)	4.21	200	0.0200
1 N_α (imid)	2.10	0.0083	1 C_β (imid)	3.10	232	0.0341
			1 C_β (imid)	3.10	128	0.0341
			1 C_γ/N_γ (imid)	4.22	195	0.8300
			1 C_γ/N_γ (imid)	4.37	159	0.8300
1 O (solv)	2.54	0.0041	1 C	3.00		0.0110

[a] Estimated errors in distances are ±0.01 Å for the first shell and ±0.03 Å for outer shells. Estimated errors in coordination numbers are ±25%. Estimated errors in angles are ±5°. ∠Cu−X−Y represents the angle between the first-shell scatterer (X) and the outer shell scatterer (Y).

zole ligand at Cu−N distances of 1.92 ± 0.01 and 2.10 ± 0.01 Å, respectively. This still leaves the 2.54 Å shell to be identified. The fits shown in Figures 2 and 3 simulate this feature with a low-Z scatterer, and both O and N give equivalent results. Second-shell assignments (S or Cl) were investigated but gave unsatisfactory fits (data not shown). We conclude that assignment of this shell to a coordinated or highly ordered water molecule is most consistent with the data. We note that, while no solvent was detected in the binuclear site in the crystal structure of the reduced mitochondrial enzyme (*13*), significant density is present between the two metals in the oxidized protein, which is consistent with either a peroxo bridge or a pair of H-bonded solvent molecules bound between Cu_B and Fe_{a3}. In support of the bound solvent hypothesis, previous EXAFS and ENDOR evidence strongly supports the presence of a water or OH^- ligand bound to Cu_B(II) in the oxidized cytochrome aa_3-600 quinol oxidase from *B. subtilis* (*11*). It is reasonable to suggest, therefore, that this solvent molecule might remain bound within the hydrophobic binuclear pocket on reduction and be weakly associated with the Cu(I) center.

Alternative fits were also examined. Given the weak outer shell scattering of the long Cu−imidazole interaction, and the difficulty of distinguishing O from N coordination by EXAFS, we tested whether a comparable fit could be obtained with the 2.10 Å shell assigned to water and the 2.5 Å shell assigned to imidazole (rather than vice versa). A fit was obtained with an F of 0.71, which was visually inferior to those shown in Figures 2 and 3 (data not shown). Attempts to simulate the data with three separate Cu−histidine interactions were also undertaken, but resulted in unreasonably small DW terms and one unusually short distance within the three Cu−N_α first-shell scatterers [Cu−N_α (DW) = 1.88 Å (0.001 Å^2), 1.99 Å (−0.001 Å^2), and 2.12 Å (0.012 Å^2); F = 0.69], but provided adequate simulation of spectral features without inclusion of any additional scattering intensity at or above 3 Å (data not shown).

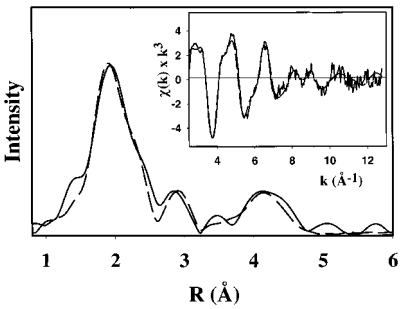

FIGURE 4: Experimental (solid lines) vs simulated (dashed lines) Fourier transform and EXAFS (inset) for reduced dark-carbonylated cytochrome bo_3 (parameters listed in Table 3).

Figure 4 shows the experimental and simulated Fourier transform and EXAFS (inset) of the reduced cytochrome bo_3 after carbonylation in the dark. The crystal structure has revealed the CO ligand tightly bound to Fe_{a3} in this derivative, with a weak association (2.5 Å) of the O atom with Cu_B (*13*). Given that we already see some low Z contribution at 2.5 Å in the fully reduced noncarbonylated enzyme, CO binding in the dark would not be expected to perturb the spectrum significantly. The results show otherwise. A major structural change occurs which produces a further broadening of the first shell, now with a distinct shoulder on the high-R side (∼2.3 Å, phase corrected), and the elimination of the 2.5 Å component of the fully reduced derivative. The EXAFS and Fourier transform are extremely

Table 3: Parameters Used To Simulate the EXAFS and Fourier Transform of the Reduced Dark-Carbonylated Cytochrome bo_3[a]

first shell			outer shells			
shell (X)	R (Å)	$2\sigma^2$ (Å^2)	shell (Y)	R (Å)	∠Cu−X−Y (deg)	$2\sigma^2$ (Å^2)
			$F = 0.413$, $E_0 = -3.06$ eV			
2 N_α (imid)	1.95	0.0134	2 C_β (imid)	2.93	236	0.0205
			2 C_β (imid)	2.95	127	0.0205
			2 C_γ/N_γ (imid)	4.15	202	0.0200
			2 C_γ/N_γ (imid)	4.27	164	0.0200
1 Cl	2.25	0.0217				

[a] Estimated errors in distances are ±0.01 Å for the first shell and ±0.03 Å for outer shells. Estimated errors in coordination numbers are ±25%. Estimated errors in angles are ±5°. ∠Cu−X−Y represents the angle between the first-shell scatterer (X) and the outer shell scatterer (Y).

reminiscent of the reduced forms of dopamine β-monooxygenase and peptidylglycine monooxygenase, both of which contain Cu(I) coordinated to two histidines at ~1.91 Å and a methionine residue at ~2.26 Å (*27*, *32*, *34*). Simulation of the bo_3 dark-carbonylated derivative converged rapidly with a coordination shell composed of two equidistant imidazole rings (single and multiple scattering with appropriate internal geometries) with a Cu−N_α scatterer (R, $2\sigma^2$) at 1.95 Å (0.0137 Å^2) and one second-shell (S or Cl) scatterer at 2.25 Å (0.0217 Å^2). The parameters used to generate this fit are listed in Table 3. Since the bo_3 sequence lacks a methionine (or cysteine) residue in a position that could coordinate Cu_B, the second-shell scatterer must be derived from chloride. Low-Z (O, N, or C) shells were totally unable to substitute for the Cl contribution. For example, a shell of one N (modeling the contribution from the third histidine ligand) refined as follows: $R = 2.05$ Å, $2\sigma^2 = 0.016$ Å^2, and $F = 0.98$, or $R = 2.62$ Å, $2\sigma^2 = 0.018$ Å^2, and $F = 1.23$. These fits were visually unacceptable, giving totally inadequate reproduction of either EXAFS or Fourier transform features.

The value of the DW term for the chloride shell (0.0217 Å^2) is larger than expected for a single first-shell scatterer, which typically would be expected to be less than 0.01 Å^2. This could occur if Cl binding were substoichiometric, leading to fractional shell occupancy. To test this possibility, we first allowed the Cl coordination number and DW term to float freely in the refinement, but the best fit was obtained at 1.3 Cl scatterers with an even higher DW of 0.0270 Å^2. When the DW was fixed at 0.0050 Å^2 and the coordination numbers for the Cl and histidine shells were both allowed to refine, the fit converged to 2.3 histidines and 0.36 Cl scatterer but with a 56% deterioration in F (from 0.40 to 0.62). Thus, the data seem to be more consistent with the alternative explanation that Cl binding is indeed stoichiometric, but the high DW term arises from a distribution of tightly bound Cl ligands among a number of different nonequivalent conformers with statically disordered Cu−Cl bond lengths.

The displacement of the 2.5 Å O or N shell by binding of CO to Fe_{o3} is interesting and supports the premise that it is derived from some ordered solvent or coordinated ligand as discussed above. Curiously, however, there is no evidence in the dark-carbonylated sample for association of the carbonyl O with Cu(I), as suggested by the crystal structure (*13*).

To gain further insight into the possible role of a coordinated halide ion in the dark-carbonylated reduced bo_3 enzyme, data were collected with a low-chloride sample in the presence and absence of bromide (see Experimental Procedures). If the chloride scatterer is derived from weakly bound adventitious Cl^-, then exhaustive dialysis should eliminate the second-row scatterer contribution. Alternatively, if it is derived from a strongly bound yet exchangeable halide ion, substitution by added bromide ion may be possible. The increased scattering magnitude and differing phase characteristics of coordinated bromide should be easily observable in the EXAFS data. The EXAFS of the Br^--treated dark-carbonylated sample is compared with that of the untreated (chloride-containing) dark-carbonylated sample depicted in Figure 1, where it can be seen to overlay on the untreated spectrum. Simulations of the low-chloride and bromide-treated samples produced essentially the same fits as those for the untreated sample. Substitution of Br for Cl produced unacceptable fits. We conclude that the Cl coordinated to Cu_B must be strongly bound to the protein and does not readily exchange with halide ions in bulk solvent.

Photolysis of the dark-carbonylated derivative is known to generate a species with CO coordinated to Cu(I) (*16*, *20*, *35*−*37*). This species differs somewhat from the widely studied Cu(I) carbonyl complexes of CuN(heterocyclic)$_3$ model complexes (*32*, *38*−*40*), which contain the thermally stable, linearly coordinated Cu−C≡O grouping with a short (1.75−1.80 Å) Cu−C bond length and a ν(C≡O) of >2070 cm^{-1}. Instead, the bo_3 Cu_B−CO complex is only transiently stable at room temperature and has a lower than expected frequency in the range of 2060−2065 cm^{-1}. In addition, FTIR clearly shows the presence of multiple conformers (*20*). Since the photolysis reaction for generating the bo_3 copper carbonyl was performed at low temperatures and is known to be one of the fastest reactions ever studied (*17*, *18*), we reasoned that CO should bind to the Cu_B center with minimal perturbation of the other ligands. In other words, we should be able to simulate the photolyzed data merely by adding the expected single and multiple scattering from one CO group to the fit for the dark-carbonylated sample.

The results of these simulations are depicted in Figure 5 with the parameters listed in Table 4. The fit is of outstanding quality, revealing two equidistant imidazole groups with a Cu−N_α distance of 2.01 Å, one chloride at 2.25 Å, and one CO with a Cu−C distance of 1.85 Å. The increase in the Cu−N(imid) bond length from 1.95 Å in the dark sample to 2.01 Å in the photolyzed sample is entirely consistent with an increase in coordination number from 3 to 4. The Cu−C(CO) distance is ~0.05 Å longer than the usual range found in model carbonyls (1.75−1.80 Å) and the Cu−O(CO) distance ~0.05 Å shorter, suggesting somewhat weakened back-bonding between Cu(I) and CO (*46*−*48*). The ability to generate a fit of this quality merely by including the scattering from a single CO ligand with the appropriate

Table 4: Parameters Used To Simulate the EXAFS and Fourier Transform of the Reduced Carbonylated Cytochrome bo_3 after Photolysis[a]

first shell			outer shells			
shell (X)	R (Å)	$2\sigma^2$ (Å^2)	shell (Y)	R (Å)	∠Cu−X−Y (deg)	$2\sigma^2$ (Å^2)
			$F = 0.391$, $E_0 = -2.66$ eV			
1 C (CO)	1.85	0.0060	1 O (CO)	2.89	150	0.0107
2 N_α (imid)	2.01	0.0077	2 C_β (imid)	2.90	238	0.0090
			2 C_β (imid)	3.09	129	0.0090
			2 C_γ/N_γ (imid)	4.17	202	0.0150
			2 C_γ/N_γ (imid)	4.29	163	0.0150
1 Cl	2.25	0.0230				

[a] Estimated errors in distances are ±0.01 Å for the first shell and ±0.03 Å for outer shells. Estimated errors in coordination numbers are ±25%. Estimated errors in angles are ±5°. ∠Cu−X−Y represents the angle between the first-shell scatterer (X) and the outer shell scatterer (Y).

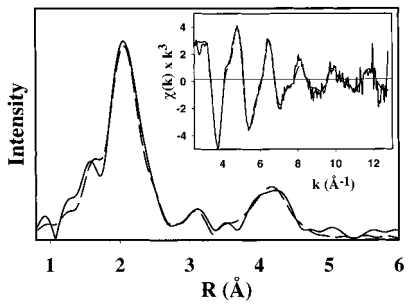

FIGURE 5: Experimental (solid lines) vs simulated (dashed lines) Fourier transform and EXAFS (inset) for reduced carbonylated cytochrome bo_3 after photolysis (parameters listed in Table 4).

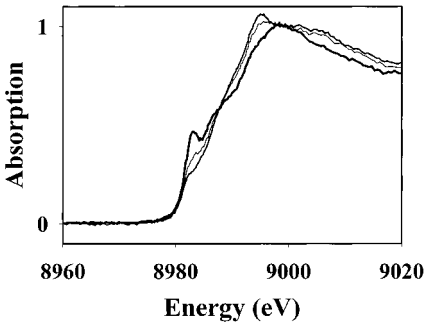

FIGURE 6: Cu K-absorption edges of fully reduced (thick line), dark-carbonylated (thin line), and photolyzed (medium line) cytochrome bo_3.

internal geometry provides additional confidence in the derived structure and, in particular, in the intimate involvement of Cl^- in the chemistry. An interesting if unexpected finding, however, is that the Cu−C−O angle appears to be considerably less than 180°, refining to 150 ± 5°. Thus CO appears to bind in a bent fashion to the copper, which may explain the deviation of the CO metrical parameters from ideal values and the thermal instability. As with the reduced, dark-carbonylated sample, the DW term for the chloride shell is high, which may again suggest multiple conformers with inequivalent Cu−Cl interactions. We note that this might provide an explanation for the multiple CO frequencies observed for Cu_B-CO.

Figure 6 shows the normalized Cu K-edges of reduced, dark-carbonylated, and photolyzed bo_3 samples (low-chloride data). All three samples exhibit a weak feature at around 8983.0 eV assigned to the 1s → 4p (and ligand shakedown) transition. The intensity of this feature is known to scale inversely with coordination number and site symmetry, the most intense features being observed for two-coordinate complexes and the weakest for four-coordinate or three-coordinate complexes axially elongated along the 3-fold axis (*41*, *42*). The fully reduced bo_3 derivative exhibits the most intense feature in the range expected for three-coordinate complexes, whereas the dark-carbonylated and photolyzed samples exhibit increasingly attenuated features, suggestive of an increase in the overall coordination number or the degree of ligation of the Cu(I) center. The absorption edges are fully consistent with the structural conclusions derived from the EXAFS analysis. The fully reduced enzyme contains two strongly coordinated ligands, the two histidines with Cu−N_α distances of 1.92 Å, while the third histidine and the 2.5 Å solvent shell are more weakly associated with the Cu(I). Dark carbonylation induces the coordination of the chloride ligand at a distance consistent with a normal bond strength, yielding a complex with three strongly bound ligands. Finally, photolysis results in the transfer of CO from Fe_{o3} to Cu_B which gives a regular four-coordinate (presumably tetrahedral) complex.

Chloride Analysis. The strong evidence for Cl coordination in dark-carbonylated and photolyzed samples, either before or after extensive dialysis of the enzyme against Cl-free media, prompted us to carry out a more detailed analysis for nondialyzable Cl ion bound to the protein. After overnight dialysis against Cl-free buffer, the enzyme preparations were diluted, filtered through a Centricon 50 centrifugal filter device, and concentrated several times, with the Cl^- concentration in the filtrate being determined each time (see Materials and Methods). When the Cl concentration of the filtrate was 20−40 μM or lower, the oxidase concentration varied between 60 and 100 μM. Then the enzyme was denatured by incubation at 100 °C for 10 min under alkaline conditions, and the solution was again placed onto the centrifugal filter. After centrifugation, the concentration of chloride was determined in the filtrate. The difference in the chloride concentration of the filtrate after and before denaturation was taken to correspond to tightly enzyme-bound chloride, which was found to be 1−2 Cl ions per bo_3 molecule. Similar experiments with the *Paracoccus* and bovine aa_3 enzymes gave results of 1 and 3.5−5 tightly bound chlorides, respectively.

DISCUSSION

Reduction of the Binuclear Site Weakens One of the Cu_B−Histidine Bonds. This study reveals for the first time that one of the three histidines that are bound to Cu_B in the oxidized enzyme at equal bond lengths (1.98 Å) becomes more loosely bound (2.10 Å) upon reduction of the binuclear site. In addition, a water molecule 2.54 Å from the copper may be weakly coordinated or highly ordered in the reduced enzyme. This may well be the same solvent molecule (OH^-

or water) that was found to be strongly bound to Cu_B at 1.90 Å in the oxidized enzyme (*11*). The latter EXAFS and ENDOR data of the structure of Cu_B in the oxidized cytochrome aa_3-600 from *B. subtilis* are in good agreement with the crystal structures of the oxidized enzyme from bovine heart mitochondria (*6*, *7*) and *P. denitrificans* (*4*, *5*), although electron density consistent with the solvent being between the heme iron and Cu_B was only found in the most recent crystallograhic study (*13*). On the other hand, it is noteworthy that the crystallographic data of the fully reduced bovine enzyme did not reveal weakening of the bond between Cu_B and one of its histidine ligands observed here.

It seems reasonable that reduction of the Cu_B site will cause protonation of an OH^- anion ligated to it, and this is also borne out by electrostatic calculations of the structure (*43*). The formed water molecule may well remain in the vicinity, possibly still weakly coordinated to Cu(I), as suggested by the data presented here. Weakening of one of the Cu−histidine bonds upon reduction of Cu(II) to Cu(I) is not unexpected from copper chemistry. A large body of structural data for Cu(I) complexes with tridentate N-donor ligands (particularly pyridyl) has established the tendency of Cu(I) to be coordinated by two strong ligands with Cu−N distances of 1.88−1.94 Å and a more distant Cu−N bond around 2.1−2.2 Å (*44*). In the more relevant imidazole systems, Sanyal and co-workers (*29*) have shown that the redox stable and O_2-inert two-coordinate $[(1,2\text{-}Me_2imid)_2\text{-}Cu(I)]^+$ binds a third equivalent of 1,2-Me_2imid to form a highly distorted three-coordinate structure with two short (1.89 Å) and one long (2.08 Å) Cu−N(imid) bond, which is now highly reactive to O_2 and forms a metastable Cu(II)−peroxo complex at −90 °C. Furthermore, weakened binding of a histidine residue on reduction has recently been observed at the Cu_A center of the M314I mutant of peptidylglycine monooxygenase (unpublished data), which is the only other known protein-bound copper center besides Cu_B in which two of the ligating histidine residues are contiguous in the sequence (*34*). The possibility that the histidine dissociation chemistry might be induced by steric strain imposed by the coordination of adjacent histidine ligands is intriguing.

Binding of CO to Heme Iron Changes the Structure of Cu_B. The binding of CO to the ferrous heme causes the loss of one of the histidine ligands of Cu_B (presumably the one that becomes loosely associated on reduction), as well as the loss of the weakly associated water molecule. In addition, Cu_B unexpectedly gains a chloride ion as a strongly bound ligand. Previous XAS studies of the heme−copper oxidases have also indicated the presence of a heavy S or Cl scatterer associated with the binuclear site metals (*45*), which has often been proposed to be the "missing" bridging ligand. After the emergence of the crystal structures, it could be stated with confidence that this scatterer was not due to a cysteine or methionine residue, or to acid-labile sulfur (*46*). Li et al. (*47*) proposed that it originated from a bound chloride ion, while Scott et al. (*48*) added credence to this suggestion by finding that the scatterer was removed from the iron EXAFS of the oxidized mitochondrial enzyme when chloride was avoided in the isolation media, and also when the enzyme was incubated with cyanide. Fann et al. (*11*) studied the copper EXAFS of the oxidized *B. subtilis* quinol oxidase and found evidence for fractional occupancy of chloride bound to Cu_B, which was independent of whether the enzyme had been dialyzed against Cl-free media. L. Powers, A. J. Moody, and P. R. Rich (personal communication) found evidence of ligation to Cu by S or Cl in the EXAFS of the oxidized bovine enzyme, irrespective of whether chloride had been specifically avoided during enzyme purification. In contrast to these EXAFS studies, which suggest a relatively strong association of chloride with the binuclear site, higher (millimolar) concentrations of chloride are required to perturb the optical heme spectrum and the cyanide binding kinetics of heme−copper oxidases (*49*), suggesting a weaker interaction.

We therefore tentatively consider Cl^- to be bound initially as an axial distal ligand of the heme iron (cf. below). At least part of the dramatic change in the structure of Cu_B accompanying heme carbonylation may be understood in view of the dynamics of CO binding to the binuclear site (*17*, *18*, *35*, *36*), according to which binding of CO to heme iron is preceded by its transient binding to Cu_B. This could already replace the histidine ligand and remove the water molecule from the immediate vicinity. When CO leaves the Cu_B, it will be unable to bind to heme iron until Cl^- dissociates. The dissociated Cl may bind to the position at Cu_B left open by the leaving CO, which binds to the ferrous heme. The fact that photodissociation of CO from heme iron to Cu_B is an extremely fast reaction (*19*) is consistent with our finding that this reaction causes no other change at Cu_B besides the addition of CO as a ligand and lengthening of the two Cu−N(imidazole) bonds.

Alternatively, the incoming CO may interact with Cu_B only by replacing the water molecule. CO may then exchange with the Cl^- bound to heme iron, as before, and it may be the binding of Cl^- to Cu_B that causes the third histidine ligand to dissociate. In this scenario, Cl^- would initially be bound to Cu_B at a position pointing toward the heme, which would not be consistent with the extremely fast binding of CO to Cu_B on photolysis, since the Cl^- remains a ligand of Cu_B after this event. Therefore, the structure of the trigonal Cu_B may change after binding of Cl^- in such a way as to move the chloride away from the heme to leave a coordination site open for fast reactivity with CO.

Although this proposal for binuclear Fe or Cu carbonylation is chemically plausible, we have not been able to locate a Cl ligand at any distance from Cu in the fully reduced enzyme. If Cl were indeed bound to Fe_{o3}, one might expect it to be observable in the Cu EXAFS around 3 Å. However, to be detectable, an atom must have some degree of correlated motion with the absorbing atom; otherwise, the DW term is too large for detection. A Cl ligand on Fe will have a spread of coordinates that is highly correlated with the Fe coordinate but totally uncorrelated with the Cu coordinate, leading to undetectability. Indeed, a single second-row scatterer at 3 Å can even be difficult to detect when it is weakly bonded to the absorber, as exemplified by the Cu−S(met) interactions in cupredoxins and cytochrome *c* oxidase Cu_A (*50*, *51*). Thus, the inability to detect Cl in the Cu K-EXAFS does not rule out an Fe−Cl interaction in the fully reduced enzyme.

Tightly Associated Chloride. Our results show that cytochrome bo_3 from *E. coli* retains at least one tightly bound chloride ion even after repetitive dialysis of the enzyme. This appears to be a chloride binding site that is considerably tighter than that previously described. Another difference is

that, whereas bromide has been shown to mimic chloride in the binding to the loose site, we could not replace chloride with bromide with respect to EXAFS-detectable binding to Cu_B.

As discussed above, in several EXAFS studies in the past, a heavy S or Cl scatterer associated with the binuclear site has been detected, and in many cases, it has been difficult to remove either by dialysis or by avoiding chloride media during isolation (see the introductory section). The distinct effects of chloride on the optical absorption spectrum and on cyanide binding kinetics (*49*), as well as the Fe EXAFS data, are suggestive of Cl^- binding to the heme iron. Interestingly, the reported Fe−Cl distance from the EXAFS is ∼2.4 Å (*46*, *48*), which may be compared with the Fe_{a3}−O distance of 2.52 Å for the bound peroxide molecule proposed by Yoshikawa et al. (*13*). The dilemma is that many of the chloride binding studies indicate only weak binding, whereas the Cu-bound chloride appears to be strongly bound in the study presented here. The situation possibly is similar to that reported by Lindberg and Andréasson (*52*) for photosystem II, where the binding of Cl^- that is responsible for high oxygen-evolving activity may appear either as high affinity with slow exchange or as low affinity with rapid exchange. It should also be noted that the strong chloride binding observed in the study presented here occurs only in the reduced carbonylated derivatives. In this regard, the ligand-induced structural change in Cu_B may be of particular interest in relation to the proposal that the proton translocation events of the heme−copper oxidases are initiated only after the binding of O_2 to the binuclear site (*53*).

Is Chloride a Cofactor? A crucial question borne out by this work is obviously whether chloride may be a cofactor in the function of the heme−copper oxidases. This work clearly establishes that CO binding to the reduced binuclear site can bring about the loss of one of the three histidine ligands of Cu_B and replacement of it by a chloride anion. A priori, this suggests that chloride is a cofactor simply because it is difficult to envisage that the active enzyme would otherwise allow for such a crucial intervention by the halide anion.

If chloride is indeed a cofactor, we would expect it to be so in most of the enzymes of the heme−copper superfamily. This is consistent with the fact that the C≡O stretching frequency of CO bound to Cu_B is virtually the same in the aa_3-type enzyme from bovine heart mitochondria and the bo_3 enzyme studied here. Cu(I) carbonyl complexes with both N_3(CO) and N_2(CO)Cl donor atom sets have been identified (*38*−*40*, *54*). A 20−30 cm^{-1} difference exists between the ν(CO) of three-coordinate copper carbonyls with N_2(CO) donor atom sets [ν(CO) > 2090 cm^{-1}] and four-coordinate copper carbonyls with N_3(CO) donor atom sets [2065 < ν(CO) < 2085 cm^{-1}]. A smaller body of literature exists for four-coordinate N_2(CO)Cl carbonyls of the type we are proposing for Cu_B, but existing data indicate frequencies in the 2060−2070-cm^{-1} range (*54*, *55*). Thus, the 2060−2065 cm^{-1} frequency observed for Cu_B is most consistent with a N_2(CO)Cl donor atom set and as such is fully consistent with the EXAFS result presented here. On the other hand, the rather small expected differences between ν(CO) for Cu(I)N_2(CO)Cl and Cu(I)N_3(CO) structures makes it difficult to draw definitive conclusions based on the CO frequencies alone.

The intimate involvement of chloride in the carbonyl transfer chemistry from Fe to Cu can also explain (at least in part) the unusual properties of the Cu_B−CO entity. The extreme thermolability of Cu_B−CO has always been enigmatic, given the availability of the three histidine ligands, and the high thermostability of Cu(I) carbonyl complexes with three N(heterocyclic) ligands in both model and enzyme systems (*27*, *32*, *38*−*40*). The EXAFS analysis indicates the likelihood of a nonlinear coordination mode for CO, which would considerably weaken the Cu−CO interaction by disrupting the back-bonding interactions. In support of this premise, the Cu−Cl bond length remains unchanged at a value (2.25 Å) more typical of three coordination in both the dark and photolyzed samples, and the Cu−C(CO) bond length (1.85 Å) is longer than expected for a terminal Cu(I)−CO, all suggestive of a rather weak association of CO with Cu_B. If, as suggested above, Cl binding reorientates the Cu_B ligand environment to leave a coordination site open for fast reactivity with CO, this may force the CO to accept a bent configuration which, though nonideal for CO binding, would be much more favorable for O_2 binding (cf. hemoglobin).

Another possibility is that Cl mimics another intrinsic anion (possibly OH^-) under the conditions of these experiments, thus possibly producing a "transition state analogue" structure of Cu_B. The evidence is clearly insufficient at the present time to conclude that Cl^- is a cofactor, but the implications of that possibility could be most interesting, for example, with respect to the proton-pumping mechanism. Therefore, more complete studies of a possible role of chloride in heme−copper oxidase function are warranted.

ACKNOWLEDGMENT

We thank Dr. Anne Puustinen for providing the purified cytochrome bo_3 from *E. coli* and gratefully acknowledge the use of facilities at the Stanford Synchrotron Radiation Laboratory (SSRL) which is supported by the National Institutes of Health Biomedical Research Technology Program, Division of Research Resources, and by the Department of Energy, Office of Biological and Environmental Research.

REFERENCES

1. Babcock, G. T., and Wikström, M. (1992) *Nature 356*, 301−309.
2. Puustinen, A., and Wikström, M. (1991) *Proc. Natl. Acad. Sci. U.S.A. 88*, 6122−6126.
3. Puustinen, A., Morgan, J. E., Verkhovsky, M., Thomas, J. W., Gennis, R. B., and Wikström, M. (1992) *Biochemistry 31*, 10363−10369.
4. Iwata, S., Ostermeier, C., Ludwig, B., and Michel, H. (1995) *Nature 376*, 660−669.
5. Ostermeier, C., Harrenga, A., Ermler, U., and Michel, H. (1997) *Proc. Natl. Acad. Sci. U.S.A. 94*, 10547−10533.
6. Tsukihara, T., Aoyama, H., Yamashita, E., Tomizaki, T., Yamaguchi, H., Shinzawa-Itoh, K., Nakashima, R., Yaono, R., and Yoshikawa, S. (1995) *Science 269*, 1069−1074.
7. Tsukihara, T., Aoyama, H., Yamashita, E., Tomizaki, T., Yamaguchi, H., Shinzawa-Itoh, K., Nakashima, R., Yaona, R., and Yoshikawa, S. (1996) *Science 272*, 1136−1144.
8. Gohlke, U., Warne, T., and Saraste, M. (1997) *EMBO J. 16*, 1181−1188.

9. Puustinen, A., Finel, M., Haltia, T., Gennis, R. B., and Wikström, M. (1991) *Biochemistry 30*, 3936−3942.
10. Hosler, J. P., Ferguson-Miller, S., Calhoun, M. W., Thomas, J. W., Hill, J., Lemieux, L., Ma, J., Georgiou, C., Fetter, J., Shapleigh, J., Tecklenburg, M. M. J., Babcock, G. T., and Gennis, R. B. (1993) *J. Bioenerg. Biomembr. 25*, 121−136.
11. Fann, Y. C., Ahmed, I., Blackburn, N. J., Boswell, J. S., Verkhovskaya, M. L., Hoffman, B. M., and Wikström, M. (1995) *Biochemistry 34*, 10245−10255.
12. van Gelder, B. F., and Beinert, H. (1969) *Biochim. Biophys. Acta 189*, 1−24.
13. Yoshikawa, S., Shinzawa-Itoh, K., Nakashima, R., Yaono, R., Yamashita, E., Inoue, N., Yao, M., Fei, M. J., Libeu, C. P., Mizushima, T., Yamaguchi, H., Tomizaki, T., and Tsukihara, T. (1998) *Science 280*, 1723−1729.
14. van Gelder, B. F. (1966) *Biochim. Biophys. Acta 118*, 36−46.
15. Steffens, G. C. M., Soulimane, T., Wolff, G., and Buse, G. (1993) *Eur. J. Biochem. 213*, 1149−1157.
16. Alben, J. O., Moh, P. P., Fiamingo, F. G., and Altschuld, R. A. (1981) *Proc. Natl. Acad. Sci. U.S.A. 78*, 234−237.
17. Dyer, R. B., Peterson, K. A., Stoutland, P. O., and Woodruff, W. H. (1991) *J. Am. Chem. Soc. 113*, 6276−6277.
18. Dyer, R. B., Peterson, K. A., Stoutland, P. O., and Woodruff, W. H. (1994) *Biochemistry 33*, 500−507.
19. Woodruff, W. H. (1993) *J. Bioenerg. Biomembr. 25*, 177−187.
20. Puustinen, A., Bailey, J. A., Dyer, R. B., Mecklenburg, S. L., Wikström, M., and Woodruff, W. H. (1997) *Biochemistry 36*, 13195−13200.
21. Morgan, J. E., Verkhovsky, M. I., Puustinen, A., and Wikström, M. (1995) *Biochemistry 34*, 15633−15637.
22. George, G. N. (1990) *EXAFSPAK*, Stanford Synchrotron Radiation Laboratory, Stanford, CA.
23. Binsted, N., Gurman, S. J., and Campbell, J. W. (1998) *EXCURV98*, Daresbury Laboratory, Daresbury, U.K.
24. Gurman, S. J. (1989) in *Synchrotron Radiation and Biophysics* (Hasnain, S. S., Ed.) pp 9−42, Ellis Horwood Ltd., Chichester, U.K.
25. Gurman, S. J., Binsted, N., and Ross, I. (1984) *J. Phys. C: Solid State Phys. 17*, 143−151.
26. Gurman, S. J., Binsted, N., and Ross, I. (1986) *J. Phys. C: Solid State Phys. 19*, 1845−1861.
27. Blackburn, N. J., Hasnain, S. S., Pettingill, T. M., and Strange, R. W. (1991) *J. Biol. Chem. 266*, 23120−23127.
28. Pettingill, T. M., Strange, R. W., and Blackburn, N. J. (1991) *J. Biol. Chem. 266*, 16996−17003.
29. Sanyal, I., Karlin, K. D., Strange, R. W., and Blackburn, N. J. (1993) *J. Am. Chem. Soc. 115*, 11259−11270.
30. Strange, R. W., Blackburn, N. J., Knowles, P. F., and Hasnain, S. S. (1987) *J. Am. Chem. Soc. 109*, 7157−7162.
31. Blackburn, N. J., Strange, R. W., Carr, R. T., and Benkovic, S. J. (1992) *Biochemistry 31*, 5298−5303.
32. Boswell, J. S., Reedy, B. J., Kulathila, R., Merkler, D. J., and Blackburn, N. J. (1996) *Biochemistry 35*, 12241−12250.
33. Dooley, D. M., Scott, R. A., Knowles, P. F., Colangelo, C. M., McGuirl, M. A., and Brown, D. E. (1998) *J. Am. Chem. Soc. 120*, 2599−2605.
34. Prigge, S. T., Kolhekar, A. S., Eipper, B. A., Mains, R. E., and Amzel, L. M. (1997) *Science 278*, 1300−1305.
35. Dyer, R. B., Einarsdottir, O., Killough, P. M., Lopez-Garriga, J. J., and Woodruff, W. H. (1989) *J. Am. Chem. Soc. 111*, 7657−7659.
36. Dyer, R. B., Lopez-Garriga, J. J., Einarsdottir, O., and Woodruff, W. H. (1989) *J. Am. Chem. Soc. 111*, 8962−8963.
37. Hosler, J. P., Kim, Y., Shapleigh, J., Gennis, R., Alben, J., Ferguson, M. S., and Babcock, G. (1994) *J. Am. Chem. Soc. 116*, 5515−5516.
38. Blackburn, N. J., Pettingill, T. M., Seagraves, K. S., and Shigeta, R. T. (1990) *J. Biol. Chem. 265*, 15383−15386.
39. Pasquali, M., and Floriani, C. (1984) in *Copper Coordination Chemistry, Biochemical and Inorganic Perspectives* (Karlin, K. D., and Zubieta, J., Eds.) pp 311−330, Adenine Press, New York.
40. Villacorta, G. M., and Lippard, S. J. (1987) *Inorg. Chem. 26*, 3672−3676.
41. Blackburn, N. J., Strange, R. W., Reedijk, J., Volbeda, A., Farooq, A., Karlin, K. D., and Zubieta, J. (1989) *Inorg. Chem. 28*, 1349−1357.
42. Kau, L. S., Spira-Solomon, D., Penner-Hahn, J. E., Hodgson, K. O., and Solomon, E. I. (1987) *J. Am. Chem. Soc. 109*, 6433−6422.
43. Kannt, A., Lancaster, C. R. D., and Michel, H. (1998) *Biophys. J. 74*, 708−721.
44. Karlin, K. D., Hayes, J. C., Gultneh, Y., Cruse, R. W., McKown, J. W., Hutchinson, J. P., and Zubieta, J. (1984) *J. Am. Chem. Soc. 106*, 2121−2128.
45. Powers, L., Chance, B., Ching, Y., and Angiolillo, P. (1981) *Biophys. J. 34*, 465−498.
46. Powers, L., Lauraeus, M., Reddy, K. S., Chance, B., and Wikström, M. (1994) *Biochim. Biophys. Acta 1183*, 504−512.
47. Li, P. M., Gelles, J., Chan, S. I., Sullivan, R. J., and Scott, R. A. (1987) *Biochemistry 26*, 2091−2095.
48. Scott, R. A., Li, P. M., and Chan, S. I. (1988) *Ann. N.Y. Acad. Sci. 550*, 53−58.
49. Moody, A. J., Butler, C. S., Watmough, N. J., Thomson, A. J., and Rich, P. R. (1998) *Biochem. J. 331*, 459−464.
50. Scott, R. A., Hahn, J. G., Doniach, S., Freeman, J. C., and Hodgson, K. O. (1982) *J. Am. Chem. Soc. 104*, 5364−5369.
51. Blackburn, N. J., de Vries, S., Barr, M. E., Houser, R. P., Tolman, W. B., Sanders, D., and Fee, J. A. (1997) *J. Am. Chem. Soc. 119*, 6135−6143.
52. Lindberg, K., and Andréasson, L. E. (1996) *Biochemistry 35*, 14259−14267.
53. Wikström, M. (1989) *Nature 338*, 776−778.
54. Ugozzoli, F., Manotti Lanfredi, A. M., Marsich, N., and Camus, A. (1997) *Inorg. Chim. Acta 256*, 1−7.
55. Pasquali, M., Floriani, C., and Gaetani-Manfredotti, A. (1981) *Inorg. Chem. 20*, 3382−3388.

BI982885L